# Supporting Information:

# Mobility of Interfaces in Silicon-based Anodes

Heesoo Park* and Alexey Y. Koposov*

*Centre for Material Science and Nanotechnology, Department of Chemistry, University of Oslo, 0371 Oslo, Norway*

E-mail: heesoo.park@smn.uio.no; alexey.koposov@kjemi.uio.no

## Details of the methods

Within the periodic cell for the $Li_xSi$/PEO simulation, there were 6 PEO chains, each composed of 28 monomers capped with methyl groups. The $Li_xSi$/DME simulation contained 756 DME molecules, matching the ether group composition in both the PEO and DME simulation boxes. The pristine amorphous Si particle was composed of 348 Si atoms and formed a spherical structure with a radius of 23 Å.

The interface between Si NP and electrolyte(s) plays a critical role in the overall stability of a particle, the mobility of Li-ions and electron transfer between active materials and surrounding media. In general, this interfacial region is known as the electric double layer (EDL),[S1] which consists of an immobile Stern layer and a mobile diffuse layer. Upon lithiation, Li-ions become chemisorbed onto Si NP surfaces, forming a compact Stern layer, while further diffusion of Li-ions in the electrolyte leads to non-uniform ion distributions in the diffuse layer. In this study, grand canonical Monte Carlo method (GCMC)[S2,S3] was used to examine the lithiation of Si NPs.

For the $Li_xSi$ anode in lithiation and delithiation, we refitted the ReaxFF parameters by

comparing the collection of geometries, equations of states, and cohesive energies between the ReaxFF and PBE-DFT calculations, based on the force fields that have successfully demonstrated active chemical reactions.[S4–S6] VASP[S7] was utilized for PBE-DFT computations. ReaxFF MD simulations were executed via LAMMPS,[S8,S9] as we performed constant pressure and temperature (NPT) integration to update each timestep (0.25 fs) for atoms using a Nose/Hoover temperature thermostat and Nose/Hoover pressure barostat, allowing anisotropic cell fluctuations. While using hybrid grand canonical Monte Carlo and molecular dynamics (GCMC/MD) method, we lithiated the Li-insertion region at the interface. All the systems were set at 1 atm pressure and a temperature of 350 K. Trajectory analysis was conducted using Ovito,[S10] which facilitated visualization and analysis.

We establish the lithium insertion area at 1.5 Å above the $Li_xSi$ surface and maintain this position at intervals of 25 ps. This approach is employed to prevent any incorporation of lithium in proximity to the electrolyte molecules that are present near the surface of the silicon nanoparticles. Variations in thickness for Li insertion, adjusting from 1.5 to 2.5 Å, only affected lithiation stages with specific capacities less than 300 mAh/g, as depicted in Figure S1. Accordingly, we established the Li insertion region at 1.5 Å above the $Li_xSi$ surface to avert Li insertion in the vicinity of the electrolyte molecules approaching the Si NP surface.

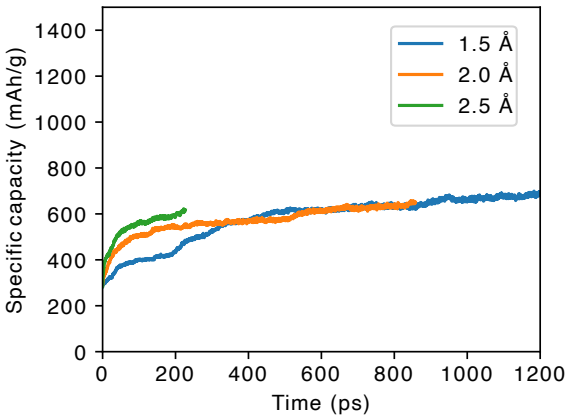


Figure S1: Lithiation of Si in PEO with the various thickness of the insertion region.

In the consecutive delithiation of $Li_xSi$, we assumed that the Li atoms present in the

electrolyte phase initially exit the diffusion layer of the EDL during the experimental process. To simulate this, we removed 100 random Li atoms from the electrolyte region every 600,000 steps (150 ps) and ensured that the Li atoms in the thin mixed layer of $Li_xSi$ and the electrolyte molecules remained unaffected, allowing structural relaxation to occur during redistribution of Li concentration. Along with the lithiated Si NPs in PEO ($Li_xSi$/PEO) and DME ($Li_xSi$/DME), we also delithiated an intermediate state (1500 mAh/g; Mid-SoC $Li_xSi$/PEO) of the lithiated Si NP. This delithiation process was done to compare the deformation of the Si NPs based on the extent of lithiation. This delithiation process was repeated until no Li atoms could be extracted for 300 ps.

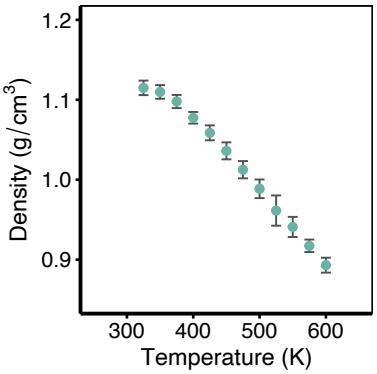


Figure S2: Density of PEO obtained by the ReaxFF MD simuilations.

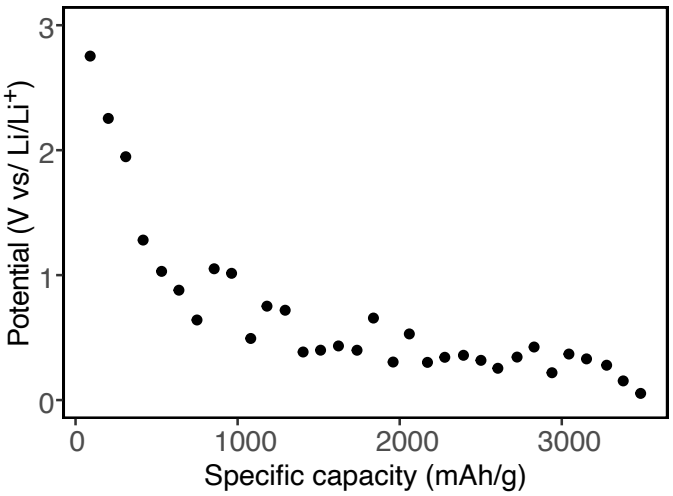


Figure S3: Voltage profile of Li-Si without electrolyte. The voltage profile was determined using ReaxFF, excluding electrolyte molecules from the simulation.

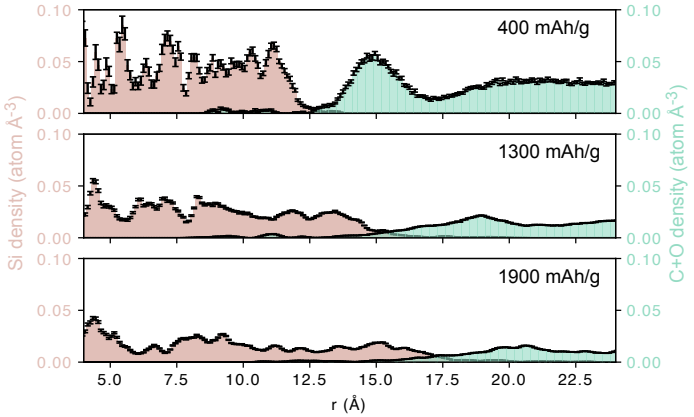


Figure S4: Number densities of silicon (Si, brown) within the Si NPs, and carbon and oxygen (C + O, green) in DME, in the lithiation, as a function of radial distance.

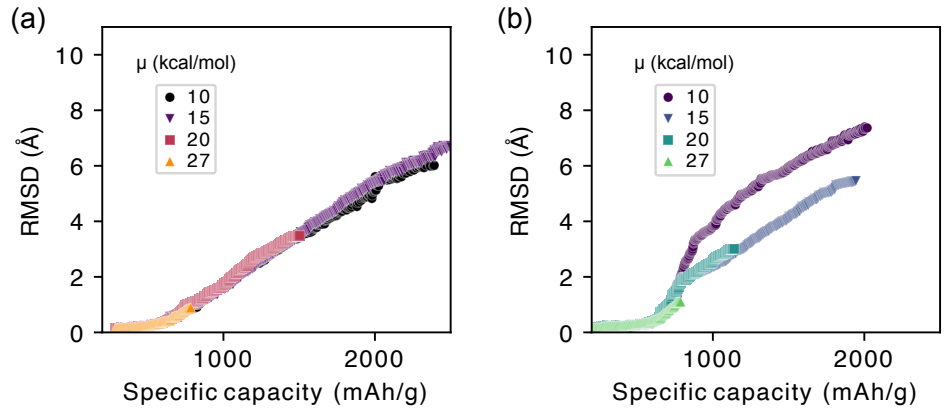


Figure S5: RMSD of the positions of the Si atoms as a functioin of the specific capacity.

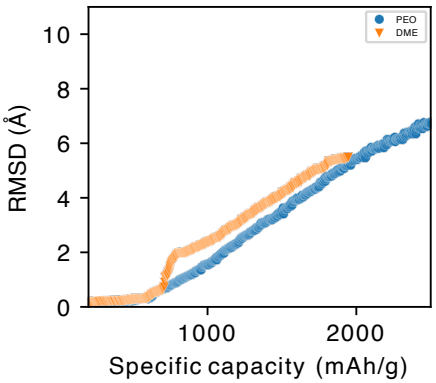


Figure S6: RMSD comparison of the positions of the Si atoms in PEO and DME at $\mu = -15$ kcal/mol.

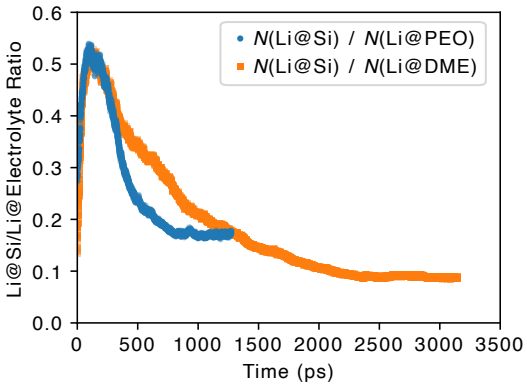


Figure S7: Comparison of the Li count in Si particles ($N$(Li@Si)) with that in PEO ($N$(Li@PEO)) and DME ($N$(Li@DME)) during lithiation at $\mu = -15$ kcal/mol.

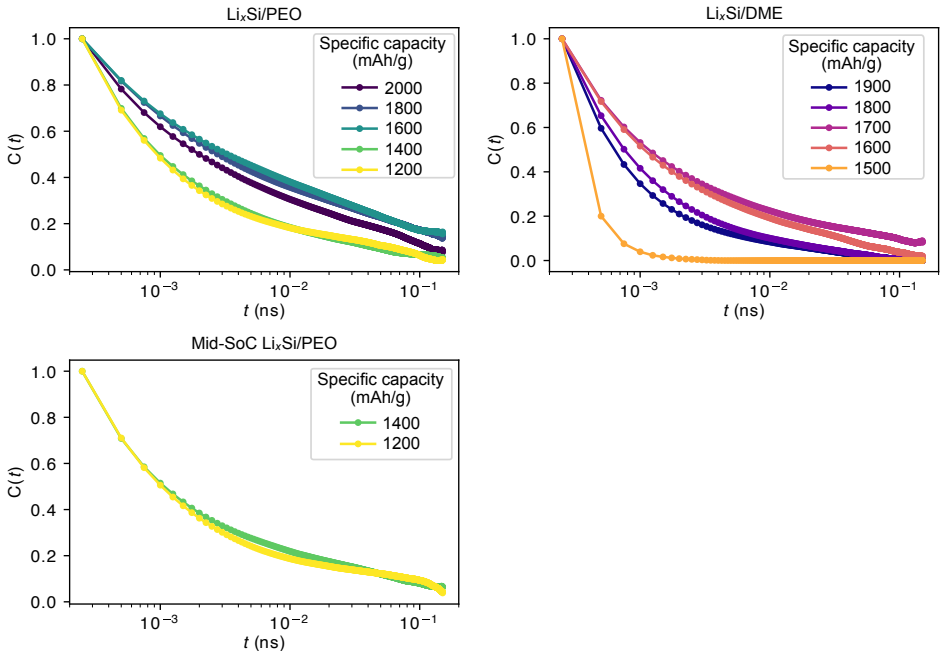


Figure S8: Time autocorrelation function of the void spaces in the PEO and DME region.

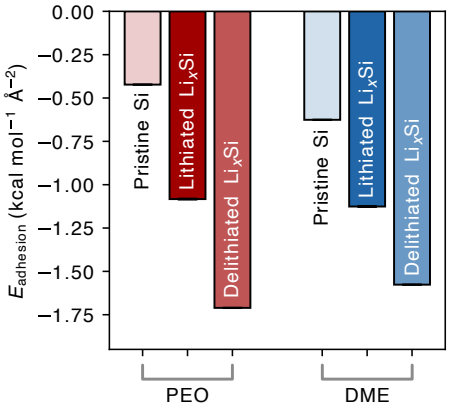


Figure S9: Adhesion energy of the PEO and DME with nanoparticles. The adhesion energy of the interface between nanoparticle (NP) and the electrolyte was calculated by $E_{\text{adhesion}} = E_{\text{NP/electrolyte}} - E_{\text{electrolyte}} - E_{\text{NP}}$, where the adhesion energy ($E_{\text{adhesion}}$) is defined as the difference in the energy of the composite system ($E_{\text{Si/binder}}$) and the individual component energies of the electrolyte molecules ($E_{\text{electrolyte}}$) and the NP ($E_{\text{NP}}$). Energy values were obtained from single-point snapshots of molecular dynamics trajectories, focusing on the instantaneous bond strength at the interface. Simulations were performed on pristine Si/PEO and Si/DME systems without lithium. Within the systems of lithiated $Li_xSi$/PEO and $Li_xSi$/DME, the electrolyte region encompasses the inserted lithium, which is a result of the lithiation process. Conversely, in the delithiated $Li_xSi$/PEO and $Li_xSi$/DME systems, the lithium is absent from the electrolyte region following the delithiation procedure having been completed. Negative values of adhesion energy ($E_{\text{adhesion}}$) indicate strong binding at the interface.

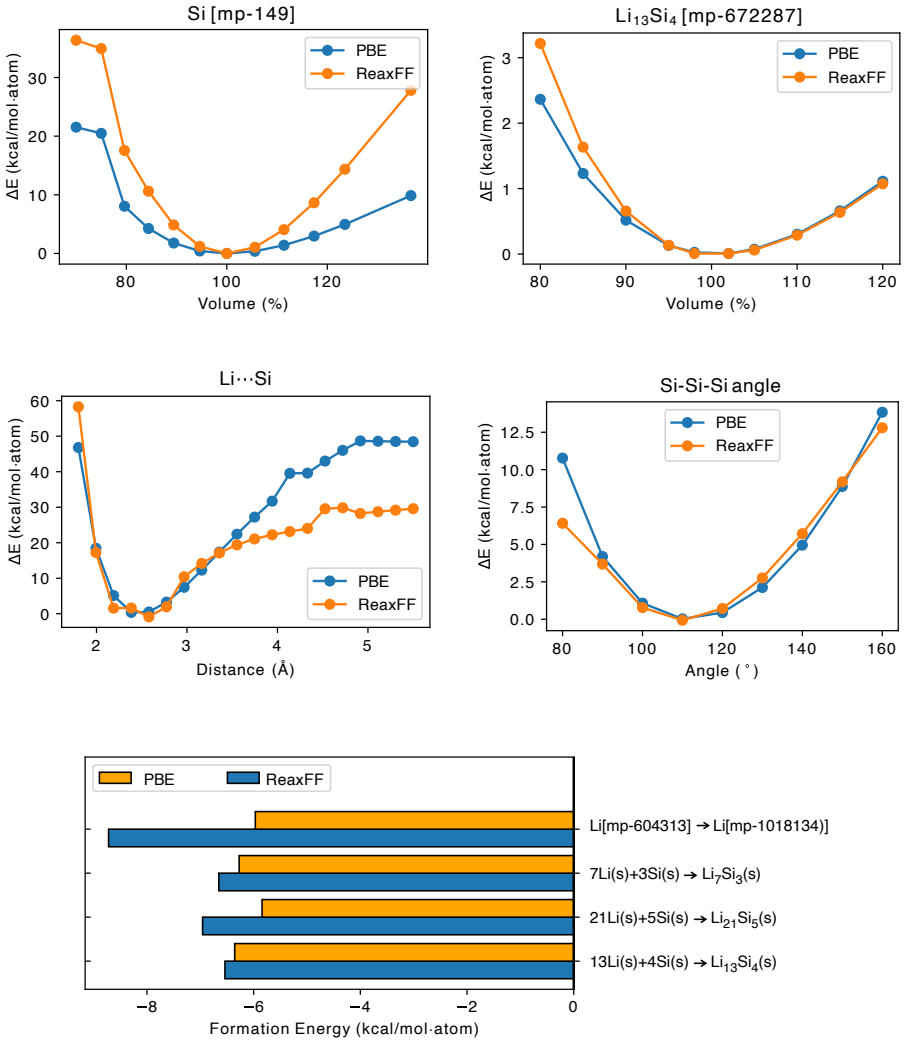


Figure S10: Comparison between DFT and ReaxFF

## ReaxFF Force Field Parameter File:

```
ForceField:C-H-O/Li/Si:PEOandDME/LixSi
 39        ! Number of general parameters
   50.0000 !p_boc1 Eq(4c): Overcoordination parame
    9.5469 !p_boc2 Eq(4d): Overcoordination parame
   26.5405 !p_coa2 Eq(15): Valency angle conjugati
    1.5105 !p_trip4 Eq(20): Triple bond stabilisat
    6.6630 !p_trip3 Eq(20): Triple bond stabilisat
   70.0000 !k_c2 Eq(19): C2-correction
    1.0588 !p_ovun6 Eq(12): Undercoordination
    4.6000 !p_trip2 Eq(20): Triple bond stabilisat
   12.1176 !p_ovun7 Eq(12): Undercoordination
   13.3056 !p_ovun8 Eq(12): Undercoordination
  -10.1292 !p_trip1 Eq(20): Triple bond stabilizat
    0.0000 !Lower Taper-radius (must be 0)
   10.0000 !R_cut Eq(21): Upper Taper-radius
    0.0000 !p_fe1 Eq(6a): Fe dimer correction
   33.8667 !p_val6 Eq(13c): Valency undercoordinat
    6.0891 !p_lp1 Eq(8): Lone pair param
    1.0563 !p_val9 Eq(13f): Valency angle exponent
    2.0384 !p_val10 Eq(13g): Valency angle paramet
    6.1431 !p_fe2 Eq(6a): Fe dimer correction
    6.9290 !p_pen2 Eq(14a): Double bond/angle para
    0.3989 !p_pen3 Eq(14a): Double bond/angle para
    3.9954 !p_pen4 Eq(14a): Double bond/angle para
    0.0000 !p_fe3 Eq(6a): Fe dimer correction
    5.7796 !p_tor2 Eq(16b): Torsion/BO parameter
```

```
  10.0000 !p_tor3 Eq(16c): Torsion overcoordinati
   1.9487 !p_tor4 Eq(16c): Torsion overcoordinati
   0.0000 !p_elho Eq(26a): electron-hole interact
   2.1645 !p_cot2 Eq(17b): Conjugation if tors13=
   1.5591 !p_vdW1 Eq(23b): vdWaals shielding
   0.1000 !Cutoff for bond order (*100)
   2.1365 !p_coa4 Eq(15): Valency angle conjugati
   0.6991 !p_ovun4 Eq(11b): Over/Undercoordinatio
  50.0000 !p_ovun3 Eq(11b): Over/Undercoordinatio
   1.8512 !p_val8 Eq(13d): Valency/lone pair para
   0.0000 !X_soft Eq(25): ACKS2 softness for X_ij
   0.0000 !d Eq(23d): Scale factor in lg-dispersi
   0.0000 !p_val Eq(27): Gauss exponent for elect
   0.0000 !1 Eq(13e): disable undecoord in val an
   2.6962 !p_coa3 Eq(15): Valency angle conjugati
 5    ! Nr of atoms; cov.r; valency;a.m;Rvdw;Evdw;gammaEEM;cov.r2;#
           alfa;gammavdW;valency;Eunder;Eover;chiEEM;etaEEM;n.u.
           cov r3;Elp;Heat inc.;bo131;bo132;bo133;softcut;n.u.
           ov/un;val1;n.u.;val3,vval4
Si   1.9948   4.0000  28.0600   2.4950   0.1289   0.8925   1.2962   4.0000
    12.3738   1.2124   4.0000  21.7115 139.9309   4.6988   6.0000   0.0000
    -1.0000   0.0000 128.2031   8.7832  23.9673   0.8381   0.8563   0.0000
    -4.6775   2.0857   1.0338   4.0000   2.5791   1.7406   0.5537  13.0125
C    1.3825   4.0000  12.0000   1.9133   0.1853   0.9000   1.1359   4.0000
     9.7602   2.1346   4.0000  33.2433  79.5548   5.8678   7.0000   0.0000
     1.2104   0.0000 199.0303   8.6991  34.7289  13.3894   0.8563   0.0000
    -2.8983   2.5000   1.0564   4.0000   2.9663   1.6737   0.1421  14.0707
```

```
H    0.7853   1.0000   1.0080   1.5904   0.0419   1.0206  -0.1000   1.0000
     9.3557   5.0518   1.0000   0.0000 121.1250   5.3200   7.4366   1.0000
    -0.1000   0.0000  54.5000   1.9771   3.3517   0.7571   1.0698   0.0000
   -15.7683   2.1488   1.0338   1.0000   2.8793   1.2669   0.0139  12.4538
O    1.2477   2.0000  15.9990   1.9236   0.0904   1.0503   1.0863   6.0000
    10.2127   7.7719   4.0000  36.9573 116.0768   8.5000   8.9989   2.0000
     0.9088   1.0003  60.8726  20.4140   3.3754   0.2702   0.9745   0.0000
    -3.6141   2.7025   1.0493   4.0000   2.9225   1.7221   0.1670  13.9991
Li   1.9814   1.0000   6.9410   1.8000   0.2939   0.9387  -0.1000   1.0000
     9.0616   1.3258   1.0000   0.0000   0.0000  -3.0000  10.0241   0.0000
    -1.0000   0.0000  37.5000   5.4409   6.9107   0.1973   0.8563   0.0000
    -2.5068   2.2989   1.0338   1.0000   2.8103   1.3000   0.2000  13.0000
15    ! Nr of bonds; Edis1;LPpen;n.u.;pbe1;pbo5;13corr;pbo6
                         pbe2;pbo3;pbo4;n.u.;pbo1;pbo2;ovcorr
 2  2 156.5953 100.0397  80.0000  -0.8157  -0.4591   1.0000  37.7369   0.4235
       0.4527  -0.1000   9.2605   1.0000  -0.0750   6.8316   1.0000   0.0000
 2  3 170.2316   0.0000   0.0000  -0.5931   0.0000   1.0000   6.0000   0.7140
       5.2267   1.0000   0.0000   1.0000  -0.0500   6.8315   0.0000   0.0000
 3  3 156.0973   0.0000   0.0000  -0.1377   0.0000   1.0000   6.0000   0.8240
       2.9907   1.0000   0.0000   1.0000  -0.0593   4.8358   0.0000   0.0000
 2  4 160.4802 105.1693  23.3059  -0.3873  -0.1613   1.0000  10.8851   1.0000
       0.5341  -0.3174   7.0303   1.0000  -0.1463   5.2913   0.0000   0.0000
 4  4  60.1463 176.6202  51.1430  -0.2802  -0.1244   1.0000  29.6439   0.9114
       0.2441  -0.1239   7.6487   1.0000  -0.1302   6.2919   1.0000   0.0000
 3  4 180.4373   0.0000   0.0000  -0.8074   0.0000   1.0000   6.0000   0.5514
       1.2490   1.0000   0.0000   1.0000  -0.0657   5.0451   0.0000   0.0000
 2  5  61.3690  -0.0200   0.0000   0.2609  -0.5000   0.0000  35.0000   0.4256
```

```
        0.8408  -0.2500  11.9965   1.0000  -0.0888   9.4023   0.0000   0.0000
 3  5  59.2034   0.0000   0.0000   0.1240   0.0000   0.0000   6.0000   0.4000
        1.0000   0.0000  12.0000   1.0000  -0.0565   4.9575   0.0000   0.0000
 4  5  70.6356  -0.0200   0.0000   0.0250   0.3000   0.0000   6.0000   0.4553
        0.8513  -0.2500  11.9965   1.0000  -0.0980   9.4453   0.0000   0.0000
 5  5  34.3154   0.0000   0.0000   0.5995   0.3000   0.0000  26.0000   0.5445
        0.5752   0.0000  12.0000   1.0000  -0.1382   4.5000   0.0000   0.0000
 2  1 106.3302  91.6240   0.0000   1.0000  -0.6097   1.0000  17.5428   0.2969
       -0.6884  -0.1271  12.2708   1.0000  -0.1438   6.2103   1.0000   0.0000
 3  1 250.5000   0.5000   0.0000  -0.7228   0.0000   1.0000   6.0000   0.3279
       15.0000   1.0000   0.0000   1.0000  -0.0744   7.4791   0.0000   0.0000
 4  1 272.8709  18.4462   0.0000  -0.6107  -0.3000   1.0000  36.0000   0.8270
       10.2334  -0.5495  29.9954   1.0000  -0.1277   7.5863   1.0000   0.0000
 1  1 108.1846  47.8775  30.0000   0.2869  -0.3320   1.0000  17.9286   0.0155
        0.0826  -0.1767   4.6243   1.0000  -0.0862   8.1051   0.0000   0.0000
 1  5  54.4890   0.0000   0.0000   1.2518  -0.8073   0.0000  19.8205   1.3574
        0.2633   0.0000  12.0000   1.0000  -0.0709   2.6826   0.0000   0.0000
10    ! Nr of off-diagonal terms; Ediss;Ro;gamma;rsigma;rpi;rpi2
 2  3   0.1219   1.4000   9.8442   1.1203  -1.0000  -1.0000
 3  4   0.0344   1.6800  10.3247   0.9013  -1.0000  -1.0000
 2  4   0.0928   1.6581   9.8390   1.2859   1.1342   1.0621
 2  5   0.0876   2.3874  11.0445   1.6854   1.0000   1.0000
 3  5   0.1149   1.4658  11.0886   1.3337  -1.0000  -1.0000
 4  5   0.3476   1.6208  10.5680   1.5144   1.0000   1.0000
 2  1   0.0963   1.0000  10.8235   1.6924   1.5790  -1.0000
 3  1   0.2367   1.5619  11.2224   1.2811  -1.0000  -1.0000
 4  1   0.2177   2.0986  10.5863   1.5766   1.3773  -1.0000
```

```
 1  5   0.1745   1.6203  20.1837   0.8112  -1.0000  -1.0000
41    ! Nr of angles;at1;at2;at3;Thetao,o;ka;kb;pv1;pv2
 2  2  2  67.2326  22.0695   1.6286   0.0000   1.7959  15.4141   1.8089
 2  2  3  65.2527  14.3185   6.2977   0.0000   0.5645   0.0000   1.1530
 3  2  3  70.0840  25.3540   3.4508   0.0000   0.0050   0.0000   3.0000
 2  3  3   0.0000   0.0000   6.0000   0.0000   0.0000   0.0000   1.0400
 2  3  2   0.0000   3.4110   7.7350   0.0000   0.0000   0.0000   1.0400
 3  3  3   0.0000  27.9213   5.8635   0.0000   0.0000   0.0000   1.0400
 2  2  4  49.5561   7.3771   4.9568   0.0000   0.7533  15.9906   1.0010
 4  2  4  77.1171  39.8746   2.5403 -24.3902   1.7740 -42.9758   2.1240
 3  2  4  65.0000  14.2057   4.8649   0.0000   0.3504   0.0000   1.7185
 2  4  2  74.3994  44.7500   0.7982   0.0000   3.0000   0.0000   1.0528
 2  4  4  77.9854  36.6201   2.0201   0.0000   0.7434  67.0264   3.0000
 4  4  4  80.7324  30.4554   0.9953   0.0000   1.6310  50.0000   1.0783
 2  4  3  71.5018  21.7062   0.4735   0.0000   0.5186   0.0000   1.1793
 3  4  4  84.9468  23.3540   1.5057   0.0000   2.6374   0.0000   1.3023
 3  4  3  77.0645  10.4737   1.2895   0.0000   0.9924   0.0000   1.1043
 2  3  4   0.0000  25.0000   3.0000   0.0000   1.0000   0.0000   1.0400
 4  3  4   0.0000   0.0148   6.0000   0.0000   0.0000   0.0000   1.0400
 3  3  4   0.0000   9.7025   6.0000   0.0000   0.0000   0.0000   1.0400
 1  1  1  77.4746  39.1276   0.8607   0.0000   0.0024   0.0000   1.2899
 3  1  1  77.2616   5.0190   7.8944   0.0000   4.0000   0.0000   1.0400
 3  1  3  75.7983  14.4132   2.8640   0.0000   4.0000   0.0000   1.0400
 4  1  1  99.8997  26.6610   2.1237   0.0000   0.0100   0.0000   1.4341
 3  1  4  73.6998  40.0000   1.8782   0.0000   4.0000   0.0000   1.1290
 4  1  4  98.2184  38.9429   0.7727   0.0000   1.1658   0.0000   2.2641
 1  4  1  39.2858   1.3068   5.6478   0.0000   3.8972   0.0000   3.0000
```

```
 3  4  1  79.2126   4.8973   8.0000   0.0000   1.0859   0.0000   2.1209
 4  4  1  82.7397  32.1198   1.8862   0.0000   0.1058   0.0000   1.5443
 3  3  1   0.0000  47.1300   6.0000   0.0000   1.6371   0.0000   1.0400
 1  3  1   0.0000  27.4206   6.0000   0.0000   1.6371   0.0000   1.0400
 4  3  1   0.0000   7.0550   3.9236   0.0000   1.6371   0.0000   1.0400
 2  2  1  72.5239  22.3583   2.0393   0.0000   1.0031   0.0000   1.0400
 2  1  2  69.1709  18.9268   2.1226   0.0000   1.0031   0.0000   1.0400
 1  2  1  68.6453  18.7377   2.0496   0.0000   1.0031   0.0000   1.0400
 2  1  1  68.9902  19.7021   2.0587   0.0000   1.0031   0.0000   1.0400
 3  2  1  72.6403  13.6964   2.4702   0.0000   1.0000   0.0000   1.0400
 2  1  3  71.8708  14.6864   2.4702   0.0000   1.0000   0.0000   1.0400
 2  4  1  85.8521  12.6881   1.0112   0.0000   1.0000   0.0000   1.3220
 2  1  4  71.7524  35.8987   1.5000   0.0000   1.0000   0.0000   1.0487
 4  2  1  70.0000   5.0250   1.0000   0.0000   1.0000   0.0000   1.2500
 2  3  1   0.0000   2.5000   1.0000   0.0000   1.0000   0.0000   1.2500
 1  1  5  76.2773  16.7449   0.8811   0.0000   0.0161   0.0000   1.0000
29    ! Nr of torsions;at1;at2;at3;at4;;V1;V2;V3;V2(BO);vconj;n.u;n
 2  2  2  2  -0.2500  11.5822   0.1879  -4.7057  -2.2047   0.0000   0.0000
 2  2  2  3  -0.2500  31.2596   0.1709  -4.6391  -1.9002   0.0000   0.0000
 3  2  2  3  -0.1770  30.0252   0.4340  -5.0019  -2.0697   0.0000   0.0000
 2  2  2  4  -0.7098  22.2951   0.0060  -2.5000  -2.1688   0.0000   0.0000
 3  2  2  4  -0.3568  22.6472   0.6045  -4.0088  -1.0000   0.0000   0.0000
 4  2  2  4  -0.0528   6.8150   0.7498  -5.0913  -1.0000   0.0000   0.0000
 2  2  4  2   2.0007  25.5641  -0.0608  -2.6456  -1.1766   0.0000   0.0000
 2  2  4  3  -1.1953  42.1545  -1.0000  -8.0821  -1.0000   0.0000   0.0000
 3  2  4  2  -0.9284  34.3952   0.7285  -2.5440  -2.4641   0.0000   0.0000
 3  2  4  3  -2.5000  79.6980   1.0000  -3.5697  -2.7501   0.0000   0.0000
```

```
2  2  4  4  -0.0179   5.0603  -0.1894  -2.5000  -2.0399   0.0000   0.0000
3  2  4  4  -0.5583  80.0000   1.0000  -4.4000  -3.0000   0.0000   0.0000
4  2  4  2  -2.5000  76.0427  -0.0141  -3.7586  -2.9000   0.0000   0.0000
4  2  4  3   0.0345  78.9586  -0.6810  -4.1777  -3.0000   0.0000   0.0000
4  2  4  4  -2.5000  66.3525   0.3986  -3.0293  -3.0000   0.0000   0.0000
2  4  4  2   2.5000  -0.5332   1.0000  -3.5096  -2.9000   0.0000   0.0000
2  4  4  3  -2.5000   3.3219   0.7180  -5.2021  -2.9330   0.0000   0.0000
3  4  4  3   2.2500  -6.2288   1.0000  -2.6189  -1.0000   0.0000   0.0000
2  4  4  4   0.0531 -17.3983   1.0000  -2.5000  -2.1584   0.0000   0.0000
3  4  4  4   0.4723 -12.4144  -1.0000  -2.5000  -1.0000   0.0000   0.0000
4  4  4  4  -2.5000 -25.0000   1.0000  -2.5000  -1.0000   0.0000   0.0000
0  2  3  0   0.0000   0.0000   0.0000   0.0000   0.0000   0.0000   0.0000
0  3  3  0   0.0000   0.0000   0.0000   0.0000   0.0000   0.0000   0.0000
0  3  4  0   0.0000   0.1000   0.0200  -2.5415   0.0000   0.0000   0.0000
0  2  2  0   0.0000  50.0000   0.3000  -4.0000  -2.0000   0.0000   0.0000
0  4  4  0   0.5511  25.4150   1.1330  -5.1903  -1.0000   0.0000   0.0000
3  1  1  3   0.0000   0.0000   0.0640  -2.4426   0.0000   0.0000   0.0000
3  1  1  1   0.0000   0.0000   0.1587  -2.4426   0.0000   0.0000   0.0000
0  3  1  0   0.0000   0.0000   0.1200  -2.4847   0.0000   0.0000   0.0000
1    ! Nr of hydrogen bonds;at1;at2;at3;Rhb;Dehb;vhb1
4  3  4   1.9682  -4.4628   1.7976   3.0000
```

# References


(S1) Wu, J. Understanding the Electric Double-Layer Structure, Capacitance, and Charging Dynamics. *Chem. Rev.* **2022**, *122*, 10821–10859.

(S2) Senftle, T. P.; Janik, M. J.; Duin, A. C. T. v. A ReaxFF Investigation of Hydride

Formation in Palladium Nanoclusters via Monte Carlo and Molecular Dynamics Simulations. *J. Phys. Chem. C* **2014**, *118*, 4967–4981.

(S3) Raju, M.; Ganesh, P.; Kent, P. R. C.; Duin, A. C. T. v. Reactive Force Field Study of Li/C Systems for Electrical Energy Storage. *J. Chem. Theory Comput.* **2015**, *11*, 2156–2166.

(S4) Liu, Y.; Sun, Q.; Yu, P.; Wu, Y.; Xu, L.; Yang, H.; Xie, M.; Cheng, T.; Goddard, W. A. I. Effects of High and Low Salt Concentrations in Electrolytes at Lithium–Metal Anode Surfaces Using DFT-ReaxFF Hybrid Molecular Dynamics Method. *J. Phys. Chem. Lett.* **2021**, *12*, 2922–2929, PMID: 33725449.

(S5) Rahnamoun, A.; van Duin, A. C. T. Reactive Molecular Dynamics Simulation on the Disintegration of Kapton, POSS Polyimide, Amorphous Silica, and Teflon during Atomic Oxygen Impact Using the Reaxff Reactive Force-Field Method. *J. Phys. Chem. A* **2014**, *118*, 2780–2787, PMID: 24679339.

(S6) Olou'ou Guifo, S. B.; Mueller, J. E.; van Duin, D.; Talkhoncheh, M. K.; van Duin, A. C. T.; Henriques, D.; Markus, T. Development and Validation of a ReaxFF Reactive Force Field for Modeling Silicon–Carbon Composite Anode Materials in Lithium-Ion Batteries. *J. Phys. Chem. C* **2023**, *127*, 2818–2834.

(S7) Kresse, G.; Furthmüller, J. Efficient iterative schemes for ab initio total-energy calculations using a plane-wave basis set. *Physical Review B* **1996**, *54*, 11169–11186.

(S8) Thompson, A. P.; Aktulga, H. M.; Berger, R.; Bolintineanu, D. S.; Brown, W. M.; Crozier, P. S.; in 't Veld, P. J.; Kohlmeyer, A.; Moore, S. G.; Nguyen, T. D.; Shan, R.; Stevens, M. J.; Tranchida, J.; Trott, C.; Plimpton, S. J. LAMMPS - a flexible simulation tool for particle-based materials modeling at the atomic, meso, and continuum scales. *Comp. Phys. Comm.* **2022**, *271*, 108171.

(S9) Aktulga, H. M.; Fogarty, J. C.; Pandit, S. A.; Grama, A. Y. Parallel reactive molecular dynamics: Numerical methods and algorithmic techniques. *Parallel Comput.* **2012**, *38*, 245–259.

(S10) Stukowski, A. Visualization and analysis of atomistic simulation data with OVITO–the Open Visualization Tool. *Modelling and Simulation in Materials Science and Engineering* **2009**, *18*, 015012.